Word count

Abstract: 212

Total word count: 4556

Number of references: 58

Number of figures: 6

Dietary fibre controls blood pressure and cardiovascular risk by lowering large intestinal pH and activating the proton-sensing receptor GPR65

Running title: Large intestinal pH, GPR65 and blood pressure

Liang Xie[1, 2], Dakota Rhys-Jones[1], Rikeish R. Muralitharan[1,3], Evany Dinakis[1], Michael Nakai[1], Madeleine Paterson[1], Alex Peh[1], Hamdi Jama[1], Ekaterina Salimova[4], Dovile Anderson[5], Caroline Ang[6], Md Jahangir Alam[2], Yu-Anne Yap[7], Darren Creek[5], Remy Robert[7], CK Yao[8], Daniel So[8], Geoffrey A. Head[9], Peter R. Gibson[8], Jane Muir[8], Joanne A. O'Donnell[1], Charles R. Mackay[2, 10], Francine Z. Marques[1, 11*]

Affiliations

[1]Hypertension Research Laboratory, School of Biological Sciences, Monash University, Clayton, VIC 3800, Australia; [2]Department of Microbiology, Biomedicine

Discovery Institute, Monash University, Clayton, VIC 3800, Australia; [3]Institute for Medical Research, Ministry of Health Malaysia, Kuala Lumpur, Malaysia; [4]Monash Biomedical Imaging, Monash University, Clayton, VIC 3168, Australia; [5]Monash Proteomics and Metabolomics Facility, Monash Institute of Pharmaceutical Sciences, Monash University, Parkville, VIC 3052, Australia; [6]Department of Biochemistry and Molecular Biology, Biomedicine Discovery Institute, Monash University, Clayton, VIC 3800, Australia; [7]Department of Physiology, Biomedicine Discovery Institute, Monash University, Clayton, VIC 3800, Australia; [8]Department of Gastroenterology, Central Clinical School, Monash University, Melbourne, 3000, Victoria, Australia; [9]Neuropharmacology Laboratory, Baker Heart and Diabetes Institute, Melbourne, 3000, Victoria, Australia; [10]School of Pharmaceutical Sciences, Shandong Analysis and Test Center, Qilu University of Technology (Shandong Academy of Sciences), Jinan, 250014, China; [11]Heart Failure Research Group Baker Heart and Diabetes Institute, Melbourne, VIC 3000, Australia.

***Corresponding author**: A/Prof Francine Z. Marques, PhD, Hypertension Research Laboratory, School of Biological Sciences, Faculty of Science, Monash University,

Melbourne, Australia, Phone: +61-03-9905 6958. E-mail: francine.marques@monash.edu

Abstract

Dietary fibre regulates blood pressure (BP) through gut microbial production of acidic metabolites known as short-chain fatty acids (SCFAs). The specific mechanisms of how SCFAs regulate BP are still emerging. We hypothesised that acidic metabolites that are abundant in the large intestine may activate proton-sensing G-protein coupled receptors, such as GPR65, thus conferring BP regulating effects. Using mouse models, we found that dietary fibre levels determined the luminal pH in the large intestine, through production of SCFAs by the gut microbiota. We then investigated a new mouse model lacking GPR65, which spontaneously developed higher BP, cardiac and renal hypertrophy and fibrosis. We identified that low pH, acting via GPR65 signalling, increased cAMP production and phosphorylation of CREB, and regulated inflammatory cytokine production involved in hypertension. We showed that the benefits of diets high in fibre, which usually prevent hypertension and its associated phenotypes, were decreased in mice lacking GPR65. Finally, we provided proof-of-concept evidence that the luminal pH profile in the colon of hypertensive participants is higher than that of normotensive participants. Colonic pH was further associated

with dietary fibre, particularly in the colonic regions where fibre is fermented by the gut microbiota. Together, we show that pH sensing by GPR65 underlies at least some of the cardiovascular benefits of dietary fibre.

Keywords: hypertension, heart, metabolites, microbiome, pH, G-protein coupled receptor

Introduction

High blood pressure (BP), known as hypertension, accounted for 19.2% of all deaths (10.8 million deaths) in 2019, primarily due to cardiovascular disease (CVD), being the leading global disease burden[1]. Insufficient intake of foods high in fibre, such as vegetables, fruits and wholegrain foods, contributes to mortality and morbidity of non-communicable diseases (NCDs)[2] resulting from higher BP and CVD[3]. Gut microbial metabolites, short-chain fatty acids (SCFAs), produced from dietary fibre fermentation, underlie the cardiovascular benefits conferred by dietary fibre[4,5]. As a consequence, dietary interventions that increase colonic SCFAs (either via direct administration or a high fibre diet) have been tested in animal studies[4,5] and, more recently, in a randomised clinical trial as a novel and safe therapy against hypertension[6]. SCFAs significantly lowered blood pressure not only in animal hypertension models[4,5], but in human non-treated essential hypertensive patients as well[7]. However, the underlying mechanism of how SCFAs lower BP remains to be fully elucidated. Thus far, studies have focused on the direct role of SCFAs, binding to GPCRs such as GPR43[4,5]. An important observation that has not been explored yet

is that the large production of SCFAs from bacterial fermentation of dietary fibre in the colon reduces the luminal pH from ~8 in the distal small intestine to ~6.5[8-10].

Acidification of the colonic pH benefits the host's health through facilitating the expansion of SCFA-producers and suppressing some gastrointestinal pathogens[11]. Nevertheless, the direct effects of the acidic luminal pH in the colon to the host's physiology remain largely unknown. The acidic intestinal pH ~6.5 created by SCFAs may activate proton-sensing receptors, including the G-protein coupled receptor GPR65[12,13]. A set of genetic variants (e.g., rs3742704, rs8005161) in the human *GPR65* gene are associated with inflammatory bowel disease (IBD)[14-19]. Indeed, GPR65-deficient mice exhibited exacerbated inflammation in experimental colitis models[19-21]. More recently, other inflammatory diseases, were associated with the *GPR65* minor T allele of rs8005161 and the minor C allele of rs3742704 in phenome-wide association studies[18,22]. These genotypes are associated with reduced GPR65 signalling, by ~50% measured by intracellular cAMP accumulation[19] and so provide an insight into the relevance of GPR65 in human disease. High BP was initially associated with rs8005161 (P=0.0029) but this was no longer significant after

adjustment by FDR (q=0.300)[18]. A potential explanation for this may be that a large proportion of hypertensive patients (41% of female patients and 51% of male patients) are not aware of their elevated BP[23]. Another explanation may be that activation of GPR65 is not due to intrinsic parameters, such as genotype, and depends on pH. Independently, GPR65 is highly expressed by various leukocyte subsets[24-26] and regulates inflammatory responses that are relevant to hypertension. For example, GPR65 inhibits the secretion of the pro-inflammatory cytokine, TNFα, which has been implicated in hypertension pathogenesis[27], from $CD4^+$ and $CD8^+$ T cells, particularly under acidic pH (pH 6.0)[18]. Thus, proton sensing by GPR65 may be an instrumental link between fibre, colonic luminal pH and cardiovascular health.

Here we aimed to establish the role of colonic pH and the proton-sensing receptor GPR65 in hypertension and its associated risk factors for CVD, particularly when fermentable fibre intake is high. We designed a series of studies in mice that provide evidence for a role of GPR65 in the cardiovascular protection conferred by dietary fibre and described the mechanism involved. Furthermore, we provided proof-of-concept that hypertensive patients have higher colonic luminal pH, compared to

normotensives, in the colonic region where dietary fibre is fermented. Collectively, we provide translational evidence that dietary fibre confers cardiovascular protection by lowering colonic pH, and activating downstream signalling of the proton-sensor GPR65 that lowers inflammatory cytokines and inflammation. This represents a novel way of gut microbiota-to-host communication and may form the basis for new therapeutic strategies for hypertension.

Results

Dietary fibre lowers large intestinal pH, and this is dependent on the gut microbiota

The large intestine, including caecum and colon, provides an anaerobic environment for the microbiota, where fermentation of dietary fibre by the microbiota releases a large amount of SCFAs, which reduce the local pH[8,9,28]. Therefore, colonic luminal pH is a quantitative marker for carbohydrate, mostly dietary fibre, fermentation by the microbiota, particularly bacteria, in the large intestine[29,30]. To determine the impact of dietary fibre on the colonic luminal pH in the large intestine, we fed C57BL/6J (wild-

type, WT) mice a control diet (AIN93G) and diets high (SF11-025) and low (SF09-028) in resistant starches (hereby referred to as 'fibre') for 7 days (Fig. 1a). As expected, these dietary interventions significantly altered the composition of the gut microbiome (Extended Data Fig. 1a-f), with SCFA producers, such as Lachnospiraceae-NK4A136-group, being enriched with the high fibre diet (Extended Data Fig. 1g). Low fibre diet significantly enriched *Alistipes* spp., which is associated with intestinal inflammation and hypertension[31,32]. The luminal pH of the caecum and colon was ~7.2 when mice were fed with the control diet (Fig. 1b). Notably, the caecal and colonic pH were reduced by high fibre diet to 6-6.5 – this was accompanied by a significant increase in the levels of acetate and total SCFAs in the colonic contents (Fig. 1c). On the contrary, low fibre diet increased the luminal pH in the caecum and colon to ~7.5 (Fig. 1b) and reduced the levels of acetate, butyrate, propionate, which together consist of more than 95% SCFAs produced in the large intestine[33], and total SCFAs in both the colonic contents and portal vein plasma relatively to the high fibre intervention (Fig. 1c). However, these short-term dietary interventions (7 days) did not alter the levels of SCFAs in the peripheral circulation

(Extended Data Fig. 1h), suggesting it is the colon where fiber intake produces marked effects.

We then aimed to determine whether the pH lowering effect of dietary fibre is dependent on the gut microbiota. To achieve this, we pre-treated mice with an antibiotic cocktail to reduce the bacteria load before we started the same dietary interventions (Fig. 1e). Indeed, the antibiotic cocktail effectively reduced the bacterial load (Fig. 1f). This reduction in bacteria in the intestine resulted in a higher luminal pH in the caecum and colon, independent of the level of fibre in the diet (Fig 1g-j). These data suggest that acidic large intestinal pH produced when fibre is consumed is dependent on the gut microbiota, particularly bacteria.

Deficiency of GPR65 results in spontaneous cardiovascular dysfunction

The colonic luminal pH produced by high fibre intake, pH 6.5, activates the family of proton-sensing GPCRs, while that produced by low fibre intake, pH 7.5, silences them[12,13]. Within this family, GPR65 has functional evidence supporting its protective roles in gut homeostasis[14-20,22]. Thus, we examined the impact of GPR65 deficiency within the gut. Using CRISPR/Cas9, we developed a new mouse strain that lacks

GPR65 (*Gpr65*$^{-/-}$). Under normal physiological conditions, *Gpr65*$^{-/-}$ mice exhibited similar gut microbiome composition (Extended Data Fig. 2a-c), immune cell infiltration (Extended Data Fig. 2d) and tissue histology in the caecum (Extended Data Fig. 2e-h) and small intestine (data not shown) compared to WT mice.

The role of GPR65 in the cardiovascular system and BP regulation remains largely unknown. Therefore, we characterized multiple key cardiovascular phenotypes of *Gpr65*$^{-/-}$ mice. Compared to WT mice, male *Gpr65*$^{-/-}$ mice had no difference in body weight (Extended Data Fig. 3a), body composition (Extended Data Fig. 3b-d), food and water intake (Extended Data Fig. 3e, f), or faeces and urine excretion (Extended Data Fig. 3g, h). We discovered, however, that *Gpr65*$^{-/-}$ mice spontaneously developed significantly higher systolic BP, diastolic BP and mean arterial pressure compared to WT mice (Fig. 2a-c). Consistently, *Gpr65*$^{-/-}$ mice had significantly enlarged heart, kidney and spleen (all adjusted to tibia length) compared to WT mice (Fig. 2d-f). This was accompanied by significantly higher levels of cardiac fibrosis (Fig. 2g, h), cardiac left ventricular posterior wall in the end diastole (LVPW;d, Fig. 2i) and cardiac output (Fig. 2j). Similarly, renal fibrosis was also significantly

elevated in *Gpr65*$^{-/-}$ mice (Fig. 2k, l). To investigate the influence of GPR65 deficiency on renal function, we performed a saline challenge as previously described[5,34]. Compared to WT mice, *Gpr65*$^{-/-}$ mice excreted less water and sodium over a 5-hour period (Fig. 2m, n), which suggests impaired diuretic and natriuretic functions. Aligned with the significant functional phenotypes, urine creatinine levels were significantly increased in *Gpr65*$^{-/-}$ mice (Fig. 2o).

We observed similar cardiovascular phenotypes in female *Gpr65*$^{-/-}$ mice, including higher BP (Extended Data Fig. 4a-c), cardiorenal and splenic hypertrophy (Extended Data Fig. 4d-f), thicker LVPW;d (Extended Data Fig. 4g), and elevated cardiorenal fibrosis (Extended Data Fig. 4h-k) compared to female WT mice. Collectively, these results clearly demonstrated that GPR65 deficiency leads to the spontaneous development of high BP and associated end-organ damage which leads to CVD.

Acidic pH regulates GPR65 signalling and inhibits pro-inflammatory pathways

A large body of evidence supports that a pro-inflammatory immune system contributes to the elevation of BP[35,36]. Considering GPR65 expression is particularly

enriched in the immune compartment[24-26], we quantified the number of immune cells in the spleen, a major lymphoid organ. Using a T cell panel (Extended Data Fig. 5a), we found that *Gpr65*$^{-/-}$ mice had significantly higher numbers of CD45^{+} immune cells (Extended Data Fig. 5b), and major T cell subsets, including CD8^{+} T cells (Fig. 3a), CD4^{+} T cells (Extended Data Fig. 5c), γδ T cells in the spleen (Extended Data Fig. 5e, f). Furthermore, we observed significantly more CCR6^{+} γδ T cells, which is a deleterious subset in CVD[37], in the spleen (Extended Data Fig. 5g-i). However, using a myeloid cell panel (Extended data Fig. 5j), we found that neutrophils and macrophages/monocytes, and dendritic cells were not enriched in the spleens of *Gpr65*$^{-/-}$ mice (Extended Data Fig. 5k-o). We then investigated the number of immune cells in kidney, a critical organ for BP regulation. Flow cytometry with the T cell panel (Extended Fig. 6a) demonstrated significantly elevated CD45^{+} immune cells (Extended Data Fig. 6b), CD8 T cells (Fig. 3b), and other major T cell subsets (Extended Data Fig. 6c-i) in the kidneys of *Gpr65*$^{-/-}$ mice. Expression of an early activation marker CD69 on T cells in kidney was not influenced by GPR65 deficiency (Fig. 4b, Extended data Fig. 6d), except on γδ T cells whose expression of CD69 was

promoted in *Gpr65*$^{-/-}$ mice (Extended data Fig. 6h). Using the myeloid cell panel (Extended data Fig. 6j), we found that neutrophils were not significantly increased in the kidneys of *Gpr65*$^{-/-}$ mice, but macrophages/monocytes, particularly Ly6C^{-} macrophages/monocytes and dendritic cells, were elevated in the kidney (Extended Data Fig. 6l-q) of *Gpr65*$^{-/-}$ mice. Thus, these data suggest *Gpr65*$^{-/-}$ mice spontaneously develop a pro-inflammatory profile that is consistent with that observed in hypertension.

We next aimed to determine whether pH modulates inflammatory responses via GPR65 signalling. GPR65 is a Gαs-coupled receptor whose activation induces intracellular cAMP accumulation[38]. cAMP production in response to low pH was impaired in macrophages of GPR65 deficient mice[39]. We discovered that low (GPR65 activating) pH (6.5) increased the level of intracellular cAMP in splenic cells in a GPR65 dependent manner (Fig. 3c). The increased intracellular cAMP can lead to the phosphorylation of cAMP response element-binding protein (CREB). Phosphorylated CREB (pCREB) has various roles in the immune responses, including suppressing the production of pro-inflammatory cytokines, IFNγ and TNFα[40], which underlie the

182 pathogenesis of hypertension[35,36]. T cells, particularly $CD8^+$ T cells, have a causal role

183 in hypertension[41]. Thus, we investigated whether pH and GPR65 signalling regulated

184 the phosphorylation of CREB in splenic T cells *in vitro*. Indeed, compared to pH 7.5,

185 pH 6.5 significantly elevated pCREB levels in WT splenic $CD8^+$ T cells activated by

186 para-Methoxyamphetamine (PMA) and ionomycin (Fig. 3d). The elevation of pCREB

187 by acidic pH was impaired in *Gpr65*$^{-/-}$ splenic $CD8^+$ T cells (Fig. 3d). In $CD4^+$ T cells,

188 acidic pH also elevated pCREB levels in WT mice but the regulation of pCREB by

189 GPR65 was not observed (Extended Data Fig. 7a). To further characterise the impact

190 of pH and GPR65 on the effector functions of T cells, we examined their influence on

191 the production of IFNγ and TNFα by $CD8^+$ T cells. pH 6.5 inhibited the production of

192 IFNγ and TNFα by stimulated splenic $CD8^+$ T cells (Fig. 3e-h) and TNFα but not

193 IFNγ production by $CD4^+$ T cells (Extended Data Fig. 7a-d) compared to pH 7.5.

194 Splenic $CD8^+$ T cells from *Gpr65*$^{-/-}$ mice produced more IFNγ and TNFα after

195 stimulation, particularly at pH 6.5 (Fig. 3e-h), but we observed no difference in $CD4^+$

196 T cells (Extended Data Fig. 7b-e), consistent with pCREB results. In summary, pH

197 change, which resembles the regulation of colonic luminal pH by dietary fibre,

regulates GPR65 signalling. Low pH, via GPR65 activation, suppresses the pro-inflammatory cytokine production by $CD8^+$ T cells, which may reduce BP (Fig. 3i).

Depletion of GPR65 decreased the protection of dietary fibre against high blood pressure

We next investigated whether pH-sensing by GPR65 conferred the cardiovascular protection by dietary fibre. To achieve this, we challenged WT and *Gpr65*$^{-/-}$ mice with angiotensin-II (Ang-II, 0.5mg/kg body/weight/day) and fed the mice either high or low fibre diets (Fig. 4a). As previously reported by us, high fibre diet suppressed the elevation of systolic BP (Fig. 4b), diastolic BP (Fig. 4c) and mean arterial pressure (Fig. 4d) induced by Ang-II infusion in WT mice[5]. Such suppression was significantly lower in *Gpr65*$^{-/-}$ mice (Fig. 4b-d, Extended Data Fig. 8a, b). GPR65 deficiency significantly increased BP with hypertensive stimuli when mice were fed with high fibre diet, while the impact of GPR65 genotype was negligible under low fibre diet (Fig. 4b-d, Extended Data Fig. 8a, b). GPR65 deficient mice treated with high fibre had higher cardiac weight to tibia length ratio (Fig. 4e), thicker LVPW;d (Fig. 4f), reduced ejection fraction (Fig. 4g) and fractional shortening (Fig. 4h), and higher

214 cardiac fibrosis (Fig. 4i, j). Similarly, kidney weight to tibia length ratio (Fig. 5a) and

215 renal fibrosis (Fig. 5b, c) were increased, but not natriuretic or diuretic function (Fig.

216 5d, e, Extended Data Fig. 8c, d). We quantified the number of immune cells in the

217 kidneys and observed that high fibre fed *Gpr65*$^{-/-}$ mice had significantly more CD45^{+}

218 immune cells compared to the high fibre fed WT mice (Fig. 5f). Of note, the

219 infiltration of CD8^{+} T cells, whose responses weas regulated by acidic pH and GPR65

220 signalling, was significantly higher in the kidney of *Gpr65*$^{-/-}$ mice (Fig. 5g). In

221 addition, γδ T cells were also increased (Fig. 5h), but there was no change in CCR6^{+}

222 γδ T cells (Fig. 5i). Macrophages/monocytes, particularly Ly6C^{-}

223 macrophages/monocytes, were increased in the kidney (Fig. 5j, k), while Ly6C^{+}

224 macrophages/monocytes, CD4^{+} T cells, Foxp3^{+} regulatory T cells, neutrophils and

225 dendritic cells were not (Fig. 5l, Extended data 8e-h). However, when mice were fed

226 with a low fibre diet, which copies a pH where GPR65 is not active, there was no

227 difference on cardiac and renal parameters besides fibrosis, which was further

228 exacerbated in *Gpr65*$^{-/-}$ mice (Fig. 4e-j, 5a-e, Extended Data Fig. 8a-d). Consistent

229 with this, no difference was observed in immune cell infiltration in the kidney under a

low fibre diet (Fig. 5f-l, Extended Data Fig. 8e-h).

We then examined the intestinal tissue of mice fed low and high fibre diets. High fibre intake thickened the muscularis propria layer and increased the length of intestinal villi in caecum, irrespective of the genotype for *Gpr65* (Extended Data Fig. 9a-c), but did not influence the width of the fibrotic layer and the number of goblet cells (Extended Data Fig. 9d, e). However, low fibre or GPR65 deficiency reduced the number of goblet cells in the duodenum (Extended Data Fig. 9f, j). We also characterized the gut microbiome composition by analysing 16S rRNA gene. The main factor driving the differences in gut microbiota was diet rather than the genotype for *Gpr65* (Extended Data Fig. 10a-e). This was also reflected in the abundance of bacterial taxa, shown at the genus level (Extended Data Fig. 10f). *Lachnospiraceae*-NK4A136-group, which was enriched by 7-day high fibre intervention (Extended Data Fig. 1g), was also more abundant in mice fed high fibre diet in this study (Extended Data Fig. 10h). The top leading taxonomic change explaining the differences in gut microbiome was the enrichment of *Bacteroides* in the groups fed high fibre diet (Extended Data Fig. 10g, h). *Bacteroides* species are the most

predominant anaerobes in the gut[42] with significant cardiovascular benefits[43-46]. Low fibre diet expanded the genera *Bilophila* and *Alistipes* (Extended Data Fig. 10g, h), associated with inflammation and higher risk of CVD.[31,32,47,48] Interestingly, *Bacteroides* spp. are the dominant carbohydrate fermenters at pH 6.0 to 7.0, the normal luminal pH within the caecum and colon.[49-51] The major products of carbohydrate fermentation by *Bacteroides* spp. are propionate and acetate, rather than butyrate[52,53]. Indeed, compared to low fibre, high fibre diet profoundly elevated acetate and propionate levels in the caecal contents, independent of the genotype of the mice, while no significant difference in caecal butyrate levels were observed (Extended Data Fig. 10i).

The intestinal luminal pH profile in human hypertension: A pilot study

To translate our experimental findings, we then examined colonic luminal pH using a wireless real-time capsule (SmartPill™) in a pilot cohort study, the pH of Intestines and Blood-pressure Regulation (pHibre) study (Fig. 6a, Extended Data Table 1). Although relative to normotensive participants, those with hypertensive had a similar total dietary fibre intake (Fig. 6b, Extended Data Table 2), dietary fibre intake of the

whole cohort was negatively associated with colonic minimum pH (Fig. 6c), but not colonic median (Fig. 6d) or maximum pH (Fig. 6e). This is important as GPR65 is activated by lower pH[13]. We discovered hypertensive patients had higher colonic minimum pH (Fig. 6f and Extended Data Table 3), without changes in maximum (Fig. 6g) or median pH (Fig. 6h). These were independent of the transit time across the small and large intestine, which were similar between groups (Extended Data Fig. 11a-c). Thus, we determined that fibre intake was associated with lower colonic minimum pH, which was higher in hypertensive compared to normotensive participants.

Most of the dietary fibre fermentation takes place in proximal colonic regions, such as the ascending and transverse colon[29]. Due to gradual reductions of dietary fibre availability, bacterial load and activity, the levels of SCFAs in the colon reduce gradually from the ascending to the descending colon; therefore, the luminal pH increases (Fig. 6i)[9,54,55]. Such pH elevation is technically difficult to be observed in small rodents, like mice, due to their small size, but can be investigated using the SmartPill™ in humans[9,56]. Thus, to study changes in pH in the different colonic

regions, we divided the colon into four equal quartiles, as previously reported[9,56] – these quartiles are thought to approximately correspond to the main regions of the large intestine. Our data indeed fitted with the expected pattern of pH distribution along the colon (Fig. 6j). Colon minimum pH was significantly correlated with the luminal pH in the first and second quartiles (Fig. 6k), consistent with higher fibre fermentation and production of SCFAs in these proximal colonic regions. We observed a non-significant increase in pH in hypertensive participants in the second quartile (P=0.157 after adjustment for age, sex and BMI). This quartile may be representative of the transverse colon, where slowly fermented fibres, such as resistant starches, are fermented[29]. These types of fibres, including resistant starch which was used in our animal studies, are a major source for SCFA-production and were shown to reduce BP in animal models[4,5] and, more recently, a human clinical trial[7].

Discussion

Dietary fibre and SCFAs are potent BP-lowering agents. SCFAs, particularly acetate,

propionate and butyrate, are well-known for their immunomodulatory effects through activation of metabolite-sensing G-protein coupled receptors (GPCRs), such as GPR41, GPR43 and GPR109A[57]. Some evidence suggests these receptors may confer cardiovascular protection[5]. Here, we used a translational approach to identify a novel mechanism of how dietary fibre regulates BP and cardiovascular health via colonic luminal pH and GPR65. Using animal models, we determined high fibre diet lowers large intestinal pH by increasing the production of SCFAs by bacteria. This change in large intestinal pH activates the proton-sensing receptor GPR65 and its downstream anti-inflammatory signalling cascade. We then used wireless real-time pH monitoring in normotensive and hypertensive participants diagnosed using ambulatory blood pressure monitoring. Consistently with our animal findings, we identified an association between human hypertension and higher colonic minimum pH. Together, our findings support that large intestinal pH-sensing by GPR65, at least partly, explains the systemic cardiovascular protection by dietary fibre.

The colon is one of the rare sites in the body where pH is naturally acidic. This largely results from the microbial production of acidic metabolites, particularly

310 SCFAs[8-10]. Acidic pH in the colon is essential in maintaining gut homeostasis through
311 suppressing the growth of pathogens and facilitating the expansion of beneficial
312 microorganisms, including SCFA producers[11]. Indeed in mice, we used dietary
313 interventions to show that fibre determined the luminal pH in the colon, and that it
314 was inversely associated with the levels of SCFAs in both the large intestine and
315 plasma. Such regulation was dependent on the existence of bacteria in the colon.
316 Moreover, we validated that total dietary fibre intake was negatively correlated with
317 the luminal pH in the first regions of the colon in participants of the pHibre cohort.

318 Among the host's pH sensors, GPR65 has critical roles in gastrointestinal
319 homeostasis[14-20,22]. In this study, we generated a new systemic GPR65 knockout
320 mouse model (*Gpr65*$^{-/-}$) using CRISPR/Cas9 technology. Aligned with a previous
321 report [21], no clear difference was observed in the gut homeostasis between naïve and
322 otherwise healthy *Gpr65*$^{-/-}$ and WT mice. However, characterisation of its
323 cardiovascular phenotype demonstrated that lack of GPR65 led to the spontaneous
324 development of cardiovascular disorders featured by higher BP, impaired cardiorenal
325 function, and cardiorenal remodelling. These results demonstrate GPR65 has a

protective role for cardiovascular health.

GPR65 is particularly enriched in immune cells and lymphoid tissues[24-26]. Evidence built in the last decade strongly support the contribution of inflammation in the development of hypertension[35,36], making hypertension an unconventional inflammatory disease. Our study suggested GPR65 deficiency increased immune cell counts in both spleen and kidneys. T cells, particularly $CD8^+$ T cells, were more abundant in *Gpr65*$^{-/-}$ mice. $CD8^+$ T cells are a well-known immune cell subset contributing to the pathogenesis of hypertension[41]. Our data demonstrated that low pH, similar as the large intestinal pH post high fibre intervention, suppresses pro-inflammatory cytokine production by $CD8^+$ T cells, but not $CD4^+$ T cells, via activating GPR65 signalling. This is a plausible mechanism linking dietary fibre, large intestinal pH, GPR65 and cardiovascular protection. $CD8^+$ T cells express GPR65 at higher levels compared to $CD4^+$ T cells[18,24], which may suggest this receptor has a more significant role in $CD8^+$ T cells rather than $CD4^+$ T cells. $CCR6^+$ γδ T cells, which are a major initial source of the pro-inflammatory cytokine IL-17A[37], were significantly more abundant in the spleens and kidneys of *Gpr65*$^{-/-}$ mice. GPR65

protects against myocardial infarction in mice, likely through suppressing IL-17A producing CCR6^{+} γδ T cells[58]. This may represent another mechanism involved in the BP regulation by GPR65, which requires further investigation. Thus, we propose that pH-sensing by GPR65 mediates the cardiovascular protection by dietary fibre via immunosuppressive mechanisms.

Our study demonstrates that the cardiovascular protection conferred by dietary fibre is, at least in part, mediated by GPR65. When challenged with Ang-II, *Gpr65*$^{-/-}$ mice had higher BP and cardiorenal hypertrophy compared to WT controls fed high fibre, and similar BP when fed a low fibre diet, which would also abort GPR65 signalling in the large intestine. Indeed, we observed that high fibre fed *Gpr65*$^{-/-}$ mice had more CD8^{+} T cells in the kidney compared to high fibre fed WT mice. Analysis of the microbiome using 16S rRNA sequencing demonstrated that diet, not *Gpr65* genotype, drove the difference in the gut microbiota composition. High fibre diet promoted *Bacteroides* spp., a genus with known cardiovascular benefits[43-46], and increased the levels of acetate and propionate, but not butyrate, in the intestine. Moreover, high fibre also inhibited certain taxa associated with inflammation and

cardiovascular disorders, including *Bilophila* and *Aliptipes*[31,32,47,48]. These data suggested that GPR65 signalling does not regulate gut microbiota composition directly and its effects in cardiovascular health are dependent on downstream pathways triggered by GPR65, such as immunomodulation as discussed above.

We acknowledge that since we used a systemic knockout model, our animal studies cannot exclude the effect of pH-sensing in other tissues. However, the interventions with low and high fibre diets show robust differences in the phenotype between WT and *Gpr65*$^{-/-}$ knockout mice that support that the importance of GPR65 signalling in hypertension starts in the colon. The *in vitro* experiments used the luminal colonic pH we determined *in vivo*; however, we acknowledge these may not correspond to colonic tissue pH. Moreover, the colonic quartiles used in the pHibre cohort analysis were based on transit time and not geography, and thus, they may not represent the exact colonic region we attempted to characterise.

In conclusion, this is the first study to report a role of luminal pH in the colon on the host's cardiovascular health in both humans and mice. We provided new insights on how dietary fibre and gut microbiota-derived metabolites regulate host health from

the perspective of pH. We established a role for GPR65 as a metabolite-sensing GPCR by sensing pH changes caused by microbial fermentations. Since pH alternation is happening universally, this mechanism through proton-sensor GPR65 may extend to broader applications. Agents reducing colonic luminal pH, or agonists activating GPR65 may be potential tools for the global control of CVDs.

Conflict of Interest

None to declare.

Acknowledgements

This study was supported by a National Heart Foundation Vanguard Grant (102927) and a National Health & Medical Research Council of Australia (NHMRC) Ideas Grant (GTN2017382). L.X., M.J.A are supported by Monash Graduate Scholarships. R.R.M is supported by a scholarship from the Faculty of Science, Monash University. J.A.O. is supported by a NHMRC Fellowship. F.Z.M is supported by a Senior Medical Research Fellowship from the Sylvia and Charles Viertel Charitable Foundation Fellowship and a National Heart Foundation Future Leader Fellowship

(105663). The Baker Heart & Diabetes Institute is supported in part by the Victorian Government's Operational Infrastructure Support Program. The authors thank Department of Gastroenterology, The Alfred, Monash Animal Research Platform, Monash Genomic Modification Platform, Monash Histology Platform, FlowCore, Monash Biomedical Imaging, Monash Proteomics and Metabolomics Facility, Department of Pathology, Monash Health, Australian Genome Research Facility for their technical supports.

Author contributions

L.X. planned and performed most of the animal in vivo and in vitro experiments, data analyses, provided intellectual inputs and wrote the manuscript. D.R.J. coordinated the pHibre and performed human data summarization, SmartPill^{TM} data analyses. R.R.M., E.D. provided major contribution to animal in vivo experiments. J.A.O. provided major contribution to pCREB detection. M.P., A.P. performed gut histology analyses. H.J. contributed to animal in vivo experiments and rodent cardiac ultrasound data analyses, heart and kidney histology analyses. E.S. performed rodent cardiac ultrasound scanning and supervised the data analyses performed by L.X.. D.A.

performed SCFA measurement by LC-MS. C.A., M.J.A., Y.A.Y. contributed to animal in vivo experiments, mouse strain maintenance and cAMP assay. D.C. supervised SCFA measurement by LC-MS. R.R. contributed to animal in vivo experiments, mouse strain maintenance and provided intellectual inputs. C.K.Y contributed pHibre study and supervised SmartPill^{TM} data analyses performed by D.R.J.. D.S., G.A.H., P.R.G., J.M. contributed to pHibre study and provided intellectual inputs. C.R.M. and F.Z.M. conceived the study and supervised the research. F.Z.M. secured the funding supporting this study. All authors approved of and contributed to the final version of the manuscript.

References

1 Murray, C. J. L. *et al.* Global burden of 87 risk factors in 204 countries and territories, 1990-2019: a systematic analysis for the Global Burden of Disease Study 2019. *The Lancet* **396**, 1223-1249, doi:10.1016/S0140-6736(20)30752-2 (2020).

2 Afshin, A. *et al.* Health effects of dietary risks in 195 countries, 1990–2017: a systematic analysis for the Global Burden of Disease Study 2017. *The Lancet* **393**, 1958-1972, doi:10.1016/S0140-6736(19)30041-8 (2019).

3 Reynolds, A. *et al.* Carbohydrate quality and human health: a series of systematic reviews and meta-analyses. *Lancet* **393**, 434-445, doi:10.1016/S0140-6736(18)31809-9 (2019).

4 Marques, F. Z. *et al.* High-Fiber Diet and Acetate Supplementation Change the Gut Microbiota and Prevent the Development of Hypertension and Heart Failure in Hypertensive Mice. *Circulation* **135**, 964-977, doi:10.1161/CIRCULATIONAHA.116.024545 (2017).

5 Kaye, D. M. *et al.* Deficiency of Prebiotic Fiber and Insufficient Signaling

Through Gut Metabolite-Sensing Receptors Leads to Cardiovascular Disease. *Circulation* **141**, 1393-1403, doi:10.1161/CIRCULATIONAHA.119.043081 (2020).

6 Rhys-Jones, D. *et al*. Microbial Interventions to Control and Reduce Blood Pressure in Australia (MICRoBIA): rationale and design of a double-blinded randomised cross-over placebo controlled trial. *Trials* **22**, 496, doi:10.1186/s13063-021-05468-2 (2021).

7 Jama, H. A. *et al*. Gut microbial metabolites lower 24-hour systolic blood pressure in untreated essential hypertensive patients. *medRxiv*, 2022.2006.2020.22276673, doi:10.1101/2022.06.20.22276673 (2022).

8 Campbell, J. M., Fahey, G. C., Jr. & Wolf, B. W. Selected indigestible oligosaccharides affect large bowel mass, cecal and fecal short-chain fatty acids, pH and microflora in rats. *J Nutr* **127**, 130-136, doi:10.1093/jn/127.1.130 (1997).

9 Cummings, J. H., Pomare, E. W., Branch, W. J., Naylor, C. P. & Macfarlane, G. T. Short chain fatty acids in human large intestine, portal, hepatic and venous

blood. *Gut* **28**, 1221, doi:10.1136/gut.28.10.1221 (1987).

10 den Besten, G. *et al.* The role of short-chain fatty acids in the interplay between diet, gut microbiota, and host energy metabolism. *Journal of Lipid Research* **54**, 2325-2340, doi:10.1194/jlr.R036012 (2013).

11 Duncan, S. H., Louis, P., Thomson, J. M. & Flint, H. J. The role of pH in determining the species composition of the human colonic microbiota. *Environ Microbiol* **11**, 2112-2122, doi:10.1111/j.1462-2920.2009.01931.x (2009).

12 Ludwig, M. G. *et al.* Proton-sensing G-protein-coupled receptors. *Nature* **425**, 93-98, doi:10.1038/nature01905 (2003).

13 Wang, J. Q. *et al.* TDAG8 is a proton-sensing and psychosine-sensitive G-protein-coupled receptor. *J Biol Chem* **279**, 45626-45633, doi:10.1074/jbc.M406966200 (2004).

14 Franke, A. *et al.* Genome-wide meta-analysis increases to 71 the number of confirmed Crohn's disease susceptibility loci. *Nat Genet* **42**, 1118-1125, doi:10.1038/ng.717 (2010).

15 Ke, X. Presence of multiple independent effects in risk loci of common complex human diseases. *Am J Hum Genet* **91**, 185-192, doi:10.1016/j.ajhg.2012.05.020 (2012).

16 Ballester, V. *et al.* Association of NOD2 and IL23R with inflammatory bowel disease in Puerto Rico. *PLoS One* **9**, e108204, doi:10.1371/journal.pone.0108204 (2014).

17 Liu, J. Z. *et al.* Association analyses identify 38 susceptibility loci for inflammatory bowel disease and highlight shared genetic risk across populations. *Nature Genetics* **47**, 979-986, doi:10.1038/ng.3359 (2015).

18 Xie, L. *et al.* pH and Proton Sensor GPR65 Determine Susceptibility to Atopic Dermatitis. *The Journal of Immunology*, ji2001363, doi:10.4049/jimmunol.2001363 (2021).

19 Lassen, K. G. *et al.* Genetic Coding Variant in GPR65 Alters Lysosomal pH and Links Lysosomal Dysfunction with Colitis Risk. *Immunity* **44**, 1392-1405, doi:10.1016/j.immuni.2016.05.007 (2016).

20 Tcymbarevich, I. *et al.* Lack of the pH-sensing Receptor TDAG8 [GPR65] in

Macrophages Plays a Detrimental Role in Murine Models of Inflammatory Bowel Disease. *J Crohns Colitis*, doi:10.1093/ecco-jcc/jjy152 (2018).

21 Chen, X. *et al.* pH sensing controls tissue inflammation by modulating cellular metabolism and endo-lysosomal function of immune cells. *Nature Immunology*, doi:10.1038/s41590-022-01231-0 (2022).

22 Diogo, D. *et al.* Phenome-wide association studies across large population cohorts support drug target validation. *Nature Communications* **9**, 4285, doi:10.1038/s41467-018-06540-3 (2018).

23 Zhou, B. *et al.* Worldwide trends in hypertension prevalence and progress in treatment and control from 1990 to 2019: a pooled analysis of 1201 population-representative studies with 104 million participants. *The Lancet* **398**, 957-980, doi:10.1016/S0140-6736(21)01330-1 (2021).

24 Heng, T. S. P. *et al.* The Immunological Genome Project: networks of gene expression in immune cells. *Nature Immunology* **9**, 1091-1094, doi:10.1038/ni1008-1091 (2008).

25 Uhlen, M. *et al.* Proteomics. Tissue-based map of the human proteome.

Science **347**, 1260419, doi:10.1126/science.1260419 (2015).

26 Thul Peter, J. *et al.* A subcellular map of the human proteome. *Science* **356**, eaal3321, doi:10.1126/science.aal3321 (2017).

27 Sriramula, S., Haque, M., Majid Dewan, S. A. & Francis, J. Involvement of Tumor Necrosis Factor-α in Angiotensin II–Mediated Effects on Salt Appetite, Hypertension, and Cardiac Hypertrophy. *Hypertension* **51**, 1345-1351, doi:10.1161/HYPERTENSIONAHA.107.102152 (2008).

28 Rubinstein, R., Howard, A. V. & Wrong, O. M. In vivo dialysis of faeces as a method of stool analysis. IV. The organic anion component. *Clin Sci* **37**, 549-564 (1969).

29 So, D., Gibson, P. R., Muir, J. G. & Yao, C. K. Dietary fibres and IBS: translating functional characteristics to clinical value in the era of personalised medicine. *Gut* **70**, 2383, doi:10.1136/gutjnl-2021-324891 (2021).

30 Farmer, A. D., Mohammed, S. D., Dukes, G. E., Scott, S. M. & Hobson, A. R. Caecal pH is a biomarker of excessive colonic fermentation. *World J Gastroenterol* **20**, 5000-5007, doi:10.3748/wjg.v20.i17.5000 (2014).

31 David, L. A. *et al*. Diet rapidly and reproducibly alters the human gut microbiome. *Nature* **505**, 559, doi:10.1038/nature12820 https://www.nature.com/articles/nature12820#supplementary-information (2013).

32 Kim, S. *et al*. Imbalance of gut microbiome and intestinal epithelial barrier dysfunction in patients with high blood pressure. *Clinical Science* **132**, 701-718, doi:10.1042/CS20180087 (2018).

33 Cook & Sellin. Review article: short chain fatty acids in health and disease. *Alimentary Pharmacology & Therapeutics* **12**, 499-507, doi:https://doi.org/10.1046/j.1365-2036.1998.00337.x (1998).

34 Kamat, N. V. *et al*. Renal transporter activation during angiotensin-II hypertension is blunted in interferon-gamma-/- and interleukin-17A-/- mice. *Hypertension* **65**, 569-576, doi:10.1161/HYPERTENSIONAHA.114.04975 (2015).

35 Drummond, G. R., Vinh, A., Guzik, T. J. & Sobey, C. G. Immune mechanisms of hypertension. *Nature Reviews Immunology*, doi:10.1038/s41577-019-0160-5 (2019).

36 Norlander, A. E., Madhur, M. S. & Harrison, D. G. The immunology of hypertension. *The Journal of Experimental Medicine* **215**, 21, doi:10.1084/jem.20171773 (2018).

37 Yan, X. *et al*. Deleterious Effect of the IL-23/IL-17A Axis and γδT Cells on Left Ventricular Remodeling After Myocardial Infarction. *Journal of the American Heart Association* **1**, e004408, doi:10.1161/JAHA.112.004408 (2012).

38 Robert, R. & Mackay, C. R. Gαs-coupled GPCRs GPR65 and GPR174. Downers for immune responses. *Immunol Cell Biol* **96**, 341-343, doi:10.1111/imcb.12027 (2018).

39 Mogi, C. *et al*. Involvement of proton-sensing TDAG8 in extracellular acidification-induced inhibition of proinflammatory cytokine production in peritoneal macrophages. *J Immunol* **182**, 3243-3251, doi:10.4049/jimmunol.0803466 (2009).

40 Wen, A. Y., Sakamoto, K. M. & Miller, L. S. The role of the transcription factor CREB in immune function. *J Immunol* **185**, 6413-6419,

doi:10.4049/jimmunol.1001829 (2010).

41 Trott, D. W. *et al.* Oligoclonal CD8+ T cells play a critical role in the development of hypertension. *Hypertension* **64**, 1108-1115, doi:10.1161/HYPERTENSIONAHA.114.04147 (2014).

42 Salyers, A. A. Bacteroides of the human lower intestinal tract. *Annual Review of Microbiology* **38**, 293-313, doi:10.1146/annurev.mi.38.100184.001453 (1984).

43 Yoshida, N. *et al*. Bacteroides vulgatus and Bacteroides dorei Reduce Gut Microbial Lipopolysaccharide Production and Inhibit Atherosclerosis. *Circulation* **138**, 2486-2498, doi:10.1161/CIRCULATIONAHA.118.033714 (2018).

44 Emoto, T. *et al*. Analysis of Gut Microbiota in Coronary Artery Disease Patients: a Possible Link between Gut Microbiota and Coronary Artery Disease. *Journal of Atherosclerosis and Thrombosis* **advpub**, doi:10.5551/jat.32672 (2016).

45 Emoto, T. *et al*. Characterization of gut microbiota profiles in coronary artery

disease patients using data mining analysis of terminal restriction fragment length polymorphism: gut microbiota could be a diagnostic marker of coronary artery disease. *Heart and Vessels* **32**, 39-46, doi:10.1007/s00380-016-0841-y (2017).

46 Karlsson, F. H. *et al.* Symptomatic atherosclerosis is associated with an altered gut metagenome. *Nature Communications* **3**, 1245, doi:10.1038/ncomms2266 (2012).

47 Qin, J. *et al.* A metagenome-wide association study of gut microbiota in type 2 diabetes. *Nature* **490**, 55-60, doi:10.1038/nature11450 (2012).

48 Devkota, S. *et al.* Dietary-fat-induced taurocholic acid promotes pathobiont expansion and colitis in Il10−/− mice. *Nature* **487**, 104-108, doi:10.1038/nature11225 (2012).

49 Walker Alan, W., Duncan Sylvia, H., McWilliam Leitch, E. C., Child Matthew, W. & Flint Harry, J. pH and Peptide Supply Can Radically Alter Bacterial Populations and Short-Chain Fatty Acid Ratios within Microbial Communities from the Human Colon. *Applied and Environmental Microbiology* **71**, 3692-

3700, doi:10.1128/AEM.71.7.3692-3700.2005 (2005).

50 Ilhan, Z. E. *et al*. pH-Mediated Microbial and Metabolic Interactions in Fecal Enrichment Cultures. *mSphere* **2**, e00047-00017, doi:doi:10.1128/mSphere.00047-17 (2017).

51 Raba, G., Adamberg, S. & Adamberg, K. Acidic pH enhances butyrate production from pectin by faecal microbiota. *FEMS Microbiology Letters* **368**, fnab042, doi:10.1093/femsle/fnab042 (2021).

52 Salonen, A. *et al*. Impact of diet and individual variation on intestinal microbiota composition and fermentation products in obese men. *The ISME Journal* **8**, 2218-2230, doi:10.1038/ismej.2014.63 (2014).

53 Aguirre, M. *et al*. Diet drives quick changes in the metabolic activity and composition of human gut microbiota in a validated in vitro gut model. *Research in Microbiology* **167**, 114-125, doi:https://doi.org/10.1016/j.resmic.2015.09.006 (2016).

54 Evans, D. F. *et al*. Measurement of gastrointestinal pH profiles in normal ambulant human subjects. *Gut* **29**, 1035-1041 (1988).

55 Macfarlane, G. T., Gibson, G. R. & Cummings, J. H. Comparison of fermentation reactions in different regions of the human colon. *J Appl Bacteriol* **72**, 57-64, doi:10.1111/j.1365-2672.1992.tb04882.x (1992).

56 Ringel-Kulka, T. *et al.* Altered Colonic Bacterial Fermentation as a Potential Pathophysiological Factor in Irritable Bowel Syndrome. *Official journal of the American College of Gastroenterology | ACG* **110** (2015).

57 Tan, J. *et al.* The role of short-chain fatty acids in health and disease. *Adv Immunol* **121**, 91-119, doi:10.1016/B978-0-12-800100-4.00003-9 (2014).

58 Nagasaka, A. *et al.* The proton-sensing G protein-coupled receptor T-cell death-associated gene 8 (TDAG8) shows cardioprotective effects against myocardial infarction. *Scientific Reports* **7**, 7812, doi:10.1038/s41598-017-07573-2 (2017).

Figures and Figure legends

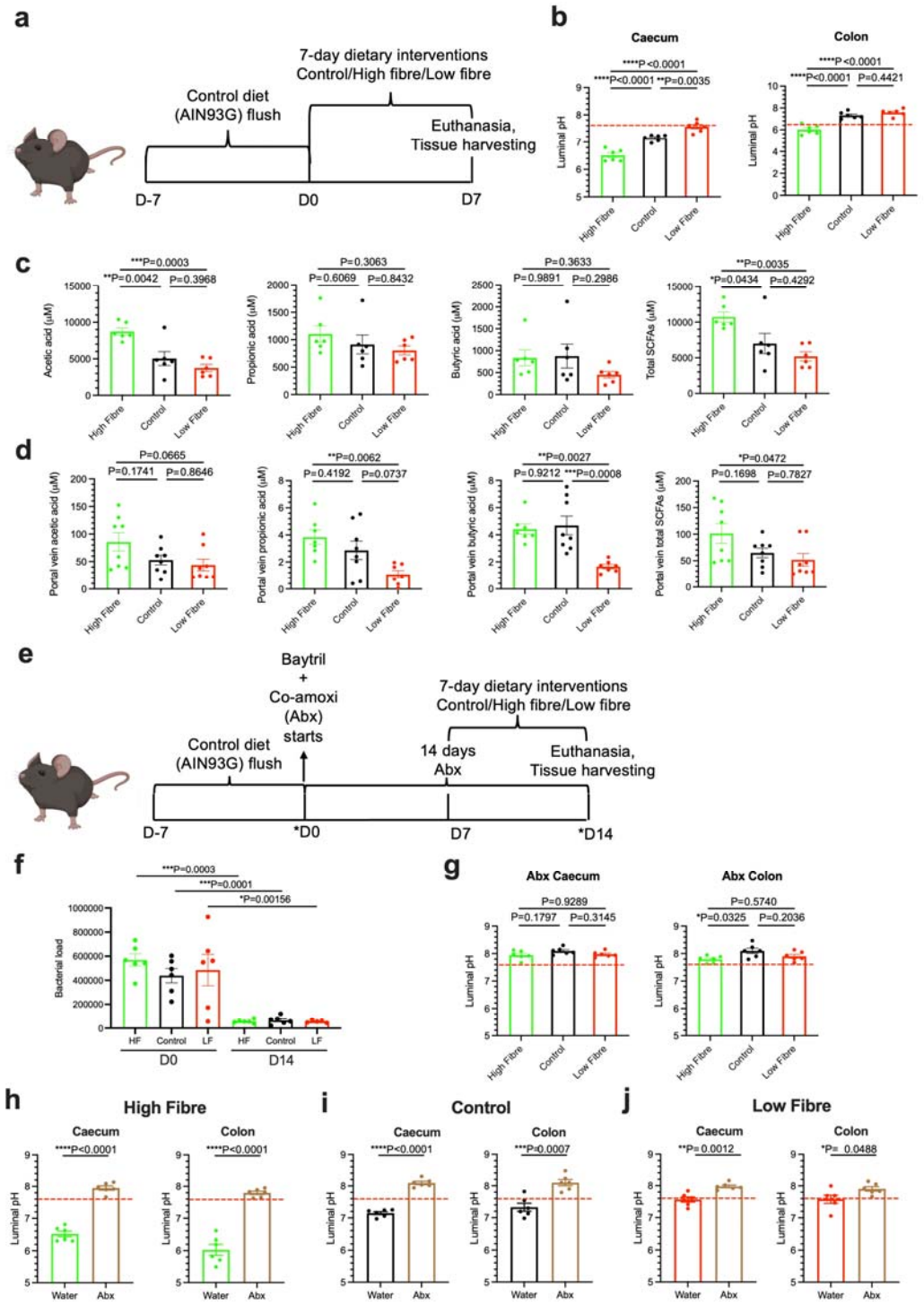

Fig. 1. Dietary fibre lowers colonic pH through the gut microbiota.

a, The experiment design to characterize the impact of dietary fibre on luminal pH in caecum and colon. **b**, Caecal and colonic luminal pH at the endpoint post dietary interventions. **c**, Levels of acetic, propionic, butyric acids and total short-chain fatty acids (SCFAs) in caecal contents. **d**, Levels of acetic, propionic, butyric acids and total SCFAs in plasma from the portal vein. **e**, The experiment design to characterize the impact of dietary fibre on luminal pH in caecum and colon with antibiotic treatment. Time points with asterisks indicates when faecal samples were collected for bacterial load measurements. **f**, Bacterial load. **g**, Caecal and colonic luminal pH at the endpoint post dietary interventions with antibiotics treatments. **h-j**, Caecal and colonic luminal pH at the endpoint post dietary interventions with/without antibiotics treatments. Each data point represents an individual mouse, and n=6 mice in each group; All data represented as means ± SEM; **c**, **d**, **g**, One-way ANOVA; **h-j**, Student's t test; *P<0.05, **P<0.01, ***P<0.001, ****P<0.0001.

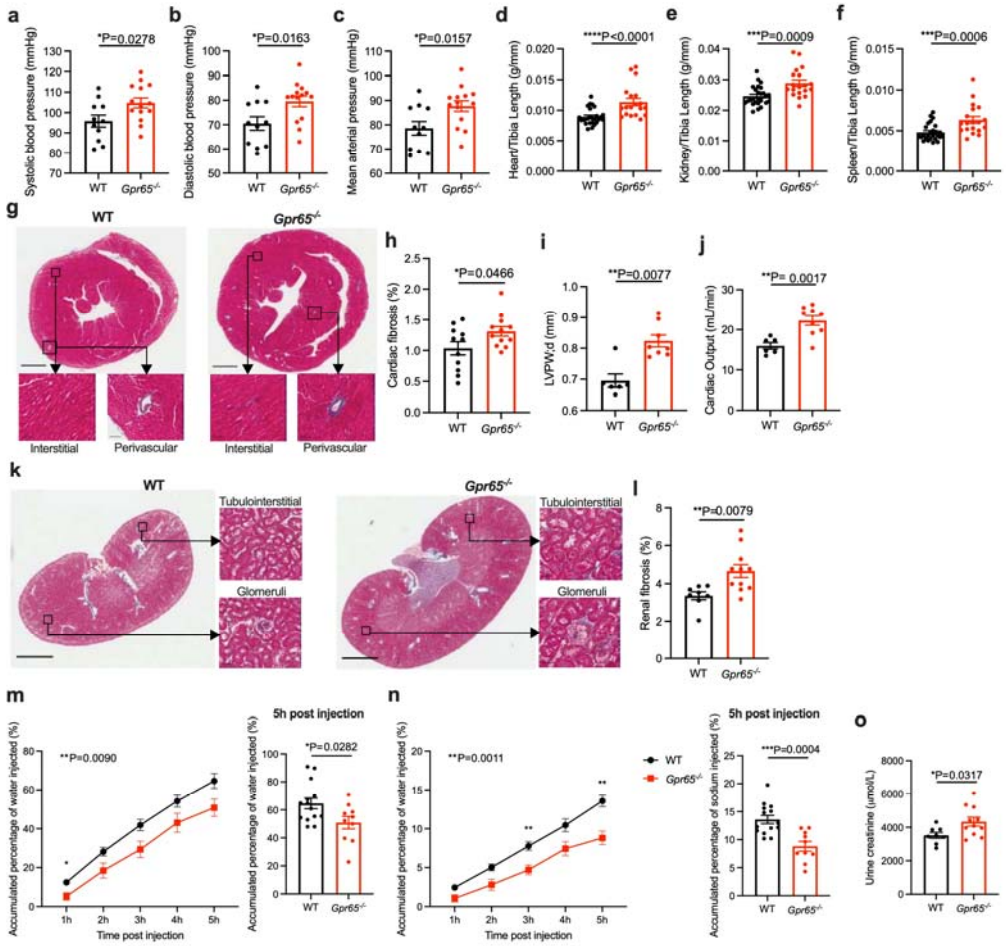

Fig. 2. GPR65 deficiency spontaneously increases tissue hypertrophy and blood pressure in male mice.

Blood pressure (BP) was measured non-invasively by tail cuff at the age of 10 weeks. **a**, Systolic BP. **b**, Diastolic BP. **c**, Mean arterial pressure. Tissues of male mice were collected and weighed at the age of 12 weeks. **d**, Heart weight to tibia length index. **e**, Kidney weight to tibia length index. **f**, Spleen weight to tibia length index. Heart sections were stained with Masson's trichrome. **g**, Representative heart sections; For

upper panels, magnification = ×10, scale bar = 1mm; For lower left panels (interstitial), magnification = ×200, scale bar = 50μm; For lower right panels (perivascular), magnification = ×100, scale bar = 100μm. **h**, Percentage of fibrotic area in the cardiac tissues. Cardiac ultrasound screening was performed at the age of 11 weeks. **i**, Left ventricle posterior wall in the end diastole. **j**, Cardiac outputs. Kidney sections were stained with Masson's trichrome. **k**, Representative kidney sections; For left panels, magnification= ×5, scale bar = 2mm; For right panels, magnification = ×200, scale bar = 50μm. **l**, Percentage of fibrotic area in the renal fibrosis. Saline challenge was performed at the age of 11 weeks. Mice were intraperitoneally injected with 10% of their body weight of 37 °C 0.9% saline solution. **m**, Renal diuretic functions measured by accumulated water excretion over 5 hours post injection. **n**, Renal natriuretic functions measured accumulated sodium excretion over 5 hours post injection. Urine samples were collected from 24h metabolic cage. **o**, The level of creatinine in urine. For the left figures of panels **m** and **n**, n=10-14 mice in each group; All data represented as means ± SEM; Two-way ANOVA. For other panels, each data point represents an individual mouse, and n=6-26 mice in each

group; All data represented as means ± SEM; **a-c**, **h**, **j**, **l** and **o**, Student's t test; **d-f**, **i**, Mann-Whitney test. *P<0.05, **P<0.01, ***P<0.001, ****P<0.0001.

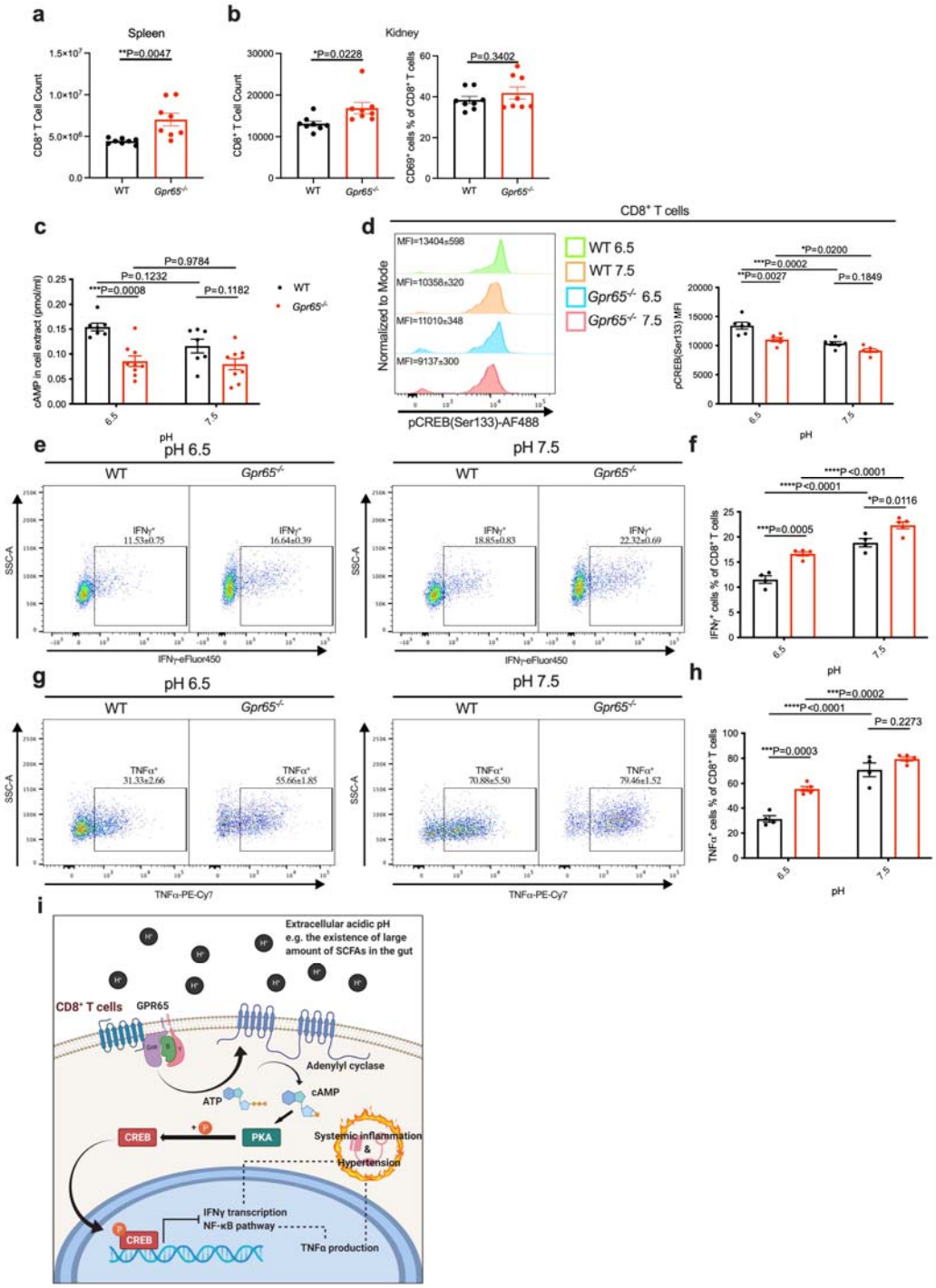

649

650 **Fig. 3. pH and GPR65 signalling modulates immune responses related to**

651 **hypertension pathogenesis.**

652 Single cell suspensions were prepared from spleens or kidneys of male mice at the

age of 12 weeks. **a**, $CD8^+$ T cell count in the spleen. **b**, $CD8^+$ T cell count and percentage of $CD69^+$ cells from $CD8^+$ T cells in the kidney. Splenocytes were isolated from mice at the age of 8-10 weeks and incubated under either pH 6.5 or pH 7.5 for 30 min. **c**, Levels of cAMP in the cell lysate extracts. 1×10^6 splenocytes were incubated with 100ng/ml PMA and 1μg/ml ionomycin for 2 hours. **d**, Representative histogram of pCREB (Ser133) levels of $CD8^+$ T cells and bar plot of pCREB (Ser133) levels of $CD8^+$ T cells. 1×10^6 splenocytes were incubated with 100ng/ml PMA and 1μg/ml ionomycin for 4 hours.1×10^6 splenocytes were incubated with 100ng/ml PMA and 1μg/ml ionomycin for 4 hours. **e**, Representative pseudocolor plots for IFNγ producing WT and *Gpr65*$^{-/-}$ $CD8^+$ T cells at pH 6.5 and 7.5 (Gated from $CD8^+$ T cells). **f**, Percentage of IFNγ producing $CD8^+$ T cells at pH 6.5 and 7.5 among WT and *Gpr65*$^{-/-}$ $CD8^+$ T cells. **g**, Representative pseudocolor plots for TNFα producing WT and *Gpr65*$^{-/-}$ $CD8^+$ T cells at pH 6.5 and 7.5 (Gated from $CD8^+$ T cells). **h**, Percentage of TNFα producing $CD8^+$ T cells at pH 6.5 and 7.5 among WT and *Gpr65*$^{-/-}$ $CD8^+$ T cells. **i**, Graphic summary of how pH regulates inflammatory responses contributing to hypertension in $CD8^+$ T cells. Created with BioRender.com. Each data point

represents an individual mouse, and n=4-9 mice in each group; All data represented as means ± SEM. **a**, **b**, Student's t test. **c**, **f**, **h**, Two-way ANOVA. *P<0.05, ***P<0.001, ***P<0.0001.

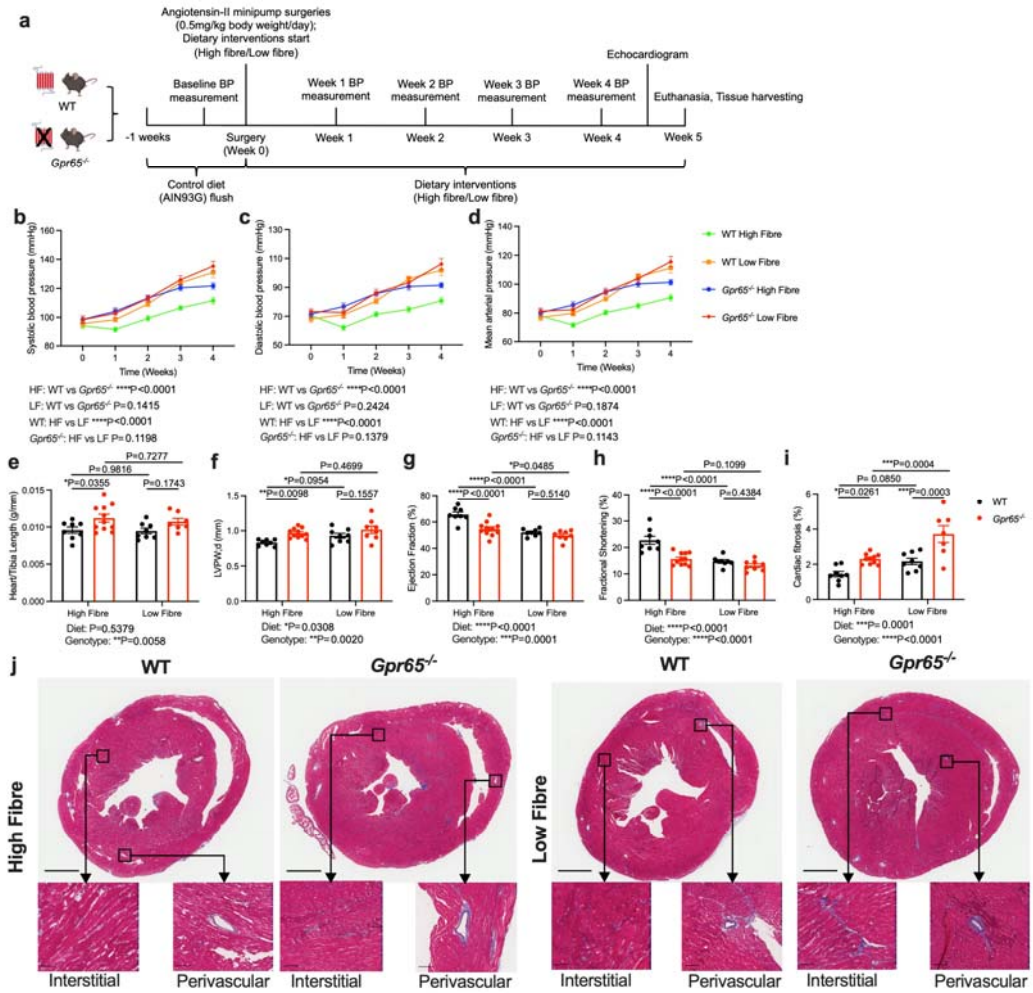

Fig. 4. Deficiency of GPR65 decreased the cardiac protective effects of dietary fibre.

6-week-old male WT and *Gpr65*$^{-/-}$ were infused with 0.5mg/kg body weight/day angiotensin-II for 28 days and fed with either HF or LF diet. **a**, The experiment design. **b**, Systolic BP profile over 4 weeks of infusion; **c**, Diastolic BP profile over 4 weeks of infusion; **d**, Mean arterial pressure profile over 4 weeks of infusion; **e**, Heart weight to tibia length index; Cardiac ultrasound scanning was performed at the week

4 of infusion. **f**, Left ventricle posterior wall in the diastole; **g**, Cardiac ejection fraction; **h**, Cardiac fractional shortening; Heart sections were stained with Masson's trichrome. **i**, Percentage of fibrotic area in the cardiac tissues. **j**, Representative heart sections; For upper panels, magnification = ×10, scale bar = 1mm; For lower left panels (interstitial), magnification = ×200, scale bar = 50μm; For lower right panels (perivascular), magnification = ×100, scale bar = 100μm. Each data point represents an individual mouse, and n=8-11 mice in each group; All data represented as means ± SEM. Two-way ANOVA. *P<0.05, **P<0.01, ***P<0.001, ****P<0.0001.

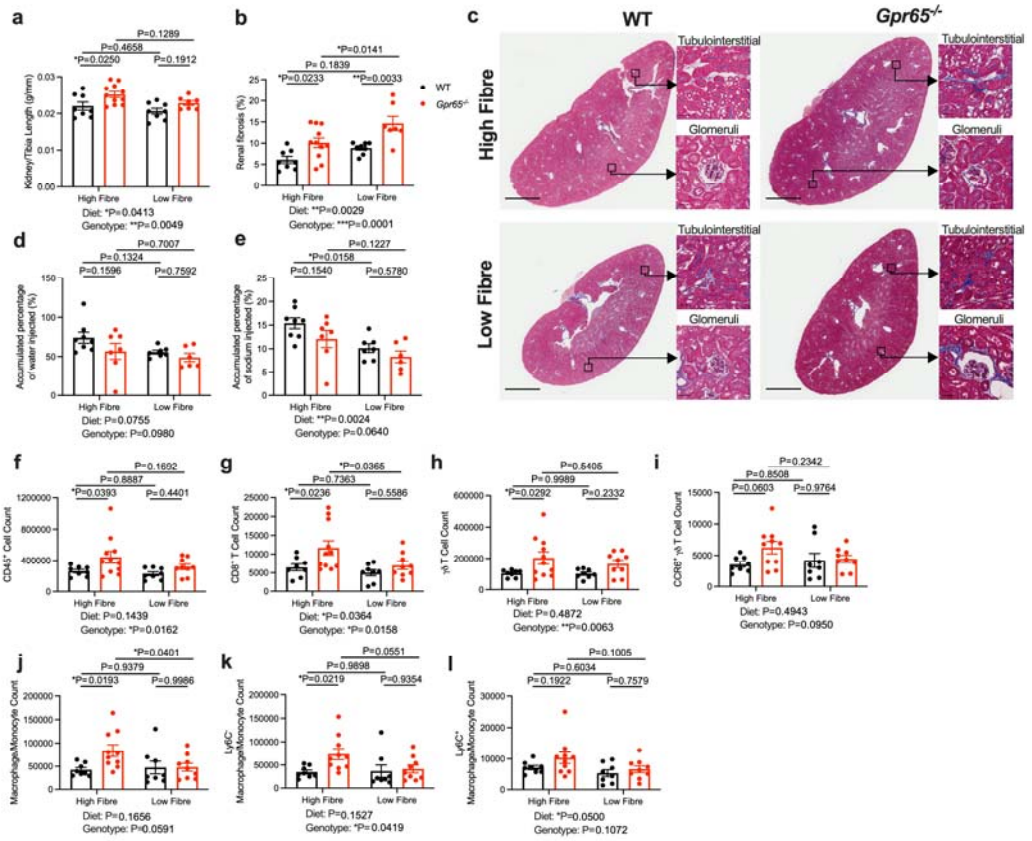

Figure 5. Deficiency of GPR65 impaired renal function and promoted renal inflammation post-hypertensive stimuli in mice fed with high fibre diet.

Kidneys were collected at the endpoint of the study. **a**, Kidney weight to tibia length index; Kidney sections were stained with Masson's trichrome. **b**, Percentage of fibrotic area in the renal tissues. **c**, Representative kidney sections; For left panels, magnification= ×5, scale bar = 2mm; For right panels, magnification = ×200, scale bar = 50μm. Mice were intraperitoneally injected with 10% of their body weight of

37 °C 0.9% saline solution at the 3rd week post minipump implantation. **d**, Renal diuretic functions measured by accumulated water excretion at the 5th hour post injection. **e**, Renal natriuretic functions measured accumulated sodium excretion at the 5th hour post injection. Single cell suspensions were prepared from kidneys of the mice at the endpoint of the study. **f**, $CD45^+$ immune cell count; **g**, $CD8^+$ T cell count; **h**, γδ T cell count; **i**, $CCR6^+$ γδ T cell count; **j**, Macrophage/Monocyte count; **k**, $Ly6C^-$ Macrophage/Monocyte count; **l**, $Ly6C^+$ Macrophage/Monocyte count. Each data point represents an individual mouse, and n=6-11 mice in each group; All data represented as means ± SEM. Two-way ANOVA. *P<0.05, **P<0.01, ***P<0.001.

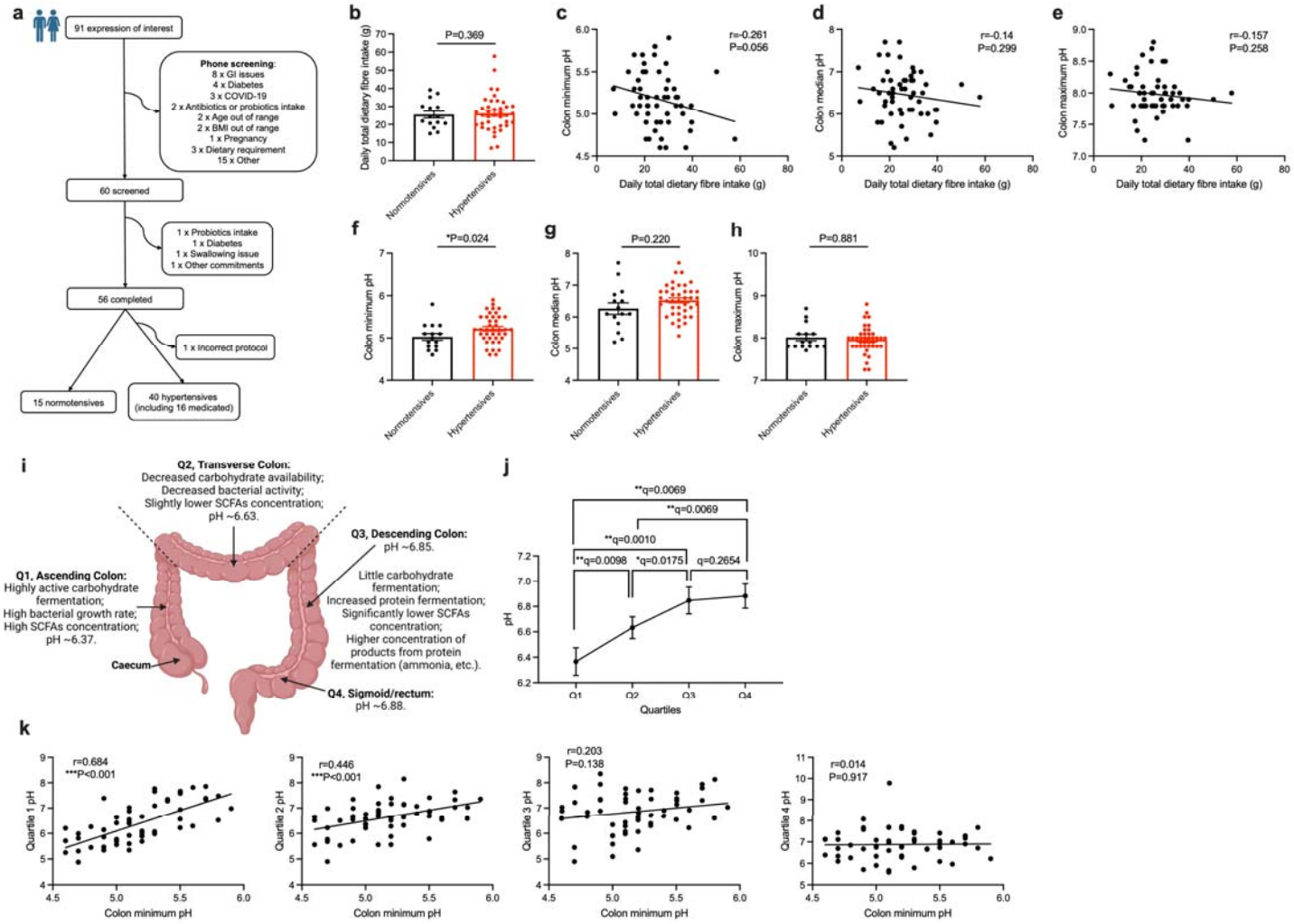
a
91 expression of interest
Phone screening:
8 x GI issues
4 x Diabetes
3 x COVID-19
2 x Antibiotics or probiotics intake
2 x Age out of range
2 x BMI out of range
1 x Pregnancy
3 x Dietary requirement
15 x Other
60 screened
1 x Probiotics intake
1 x Diabetes
1 x Swallowing issue
1 x Other commitments
56 completed
1 x Incorrect protocol
15 normotensives
40 hypertensives (including 16 medicated)
b
P=0.369
Daily total dietary fibre intake (g)
Normotensives
Hypertensives
c
r=-0.261
P=0.056
Colon minimum pH
Daily total dietary fibre intake (g)
d
r=-0.14
P=0.299
Colon median pH
Daily total dietary fibre intake (g)
e
r=-0.157
P=0.258
Colon maximum pH
Daily total dietary fibre intake (g)
f
*P=0.024
Colon minimum pH
Normotensives
Hypertensives
g
P=0.220
Colon median pH
Normotensives
Hypertensives
h
P=0.881
Colon maximum pH
Normotensives
Hypertensives
i
Q2, Transverse Colon:
Decreased carbohydrate availability;
Decreased bacterial activity;
Slightly lower SCFAs concentration;
pH ~6.63.
Q3, Descending Colon:
pH ~6.85.
Little carbohydrate fermentation;
Increased protein fermentation;
Significantly lower SCFAs concentration;
Higher concentration of products from protein fermentation (ammonia, etc.).
Q1, Ascending Colon:
Highly active carbohydrate fermentation;
High bacterial growth rate;
High SCFAs concentration;
pH ~6.37.
Caecum
Q4, Sigmoid/rectum:
pH ~6.88.
j
**q=0.0069
**q=0.0069
**q=0.0010
**q=0.0098
*q=0.0175
q=0.2654
pH
Q1
Q2
Q3
Q4
Quartiles
k
r=0.684
***P<0.001
Quartile 1 pH
Colon minimum pH
r=0.446
***P<0.001
Quartile 2 pH
Colon minimum pH
r=0.203
P=0.138
Quartile 3 pH
Colon minimum pH
r=0.014
P=0.917
Quartile 4 pH
Colon minimum pH

706

Fig. 6. The intraluminal pH profile within the colon of normotensive and hypertensive participants.

a, Recruitment summary. Out of 91 expressions of interest, 55 participants have finished the trial so far. GI, gastrointestine; COVID, coronavirus disease; BMI, body mass index; BP, blood pressure. The demographic summary and the relevant clinical information collected at the initial screening is in Extended Data Table 1. **b**, Daily total dietary fibre intake. **c-e**, Correlations of daily total dietary fibre intake with colon minimum, median and maximum pH generated by the SmartPill^{TM}, showing that fibre intake affected the colonic minimum pH the most. **f**, Colon minimum pH, **g**, colon median pH, and **h**, colon maximum pH in normotensive (n=15) versus hypertensive participants (n=40). **i,** Graphic scheme of regional pH profile in colon and respective bacterial activity, short-chain fatty acids (SCFAs) concentration. Adapted from [9,55] (Created with BioRender.com). **j**, Regional pH profile in the colon of the pHibre cohort generated by the SmartPill^{TM}. **k**, Correlations of colon minimum pH with luminal pH in different quartiles of colon. Each data point represents an individual participant. All data represented as mean ± SEM; P-values from correlations, one-way ANOVA, or regression analysis adjusted for sex, age and BMI (n=55).

717